Influence of Sleeper Base Area and Spacing on Long-Term Differential Settlement in a Railway Track Transition Zone

K. Nasrollahi and J. Nielsen

Department of Mechanics and Maritime Sciences, Chalmers University of Technology
Gothenburg, Sweden

Abstract

A model for simulation of track geometry degradation is demonstrated by predicting and comparing the long-term performance of three transition zone designs in terms of differential settlement and voided sleepers. It includes a calibrated two-dimensional (2D) finite element model of a transition zone between a ballasted track on an embankment and a slab track on a rigid foundation. The influence of using shorter sleeper spacing or a broader sleeper base design to reduce the track stiffness gradient between the two track forms and improve the dynamic vehicle–track interaction is evaluated. The 2D track model includes a state-dependent seven-parameter model of the ballast and subgrade, accounting for potential loss of contact between sleepers and ballast and the interaction between sleepers via the ground, while the vehicle model represents a heavy haul wagon with axle loads 30 tonnes and speed 60 km/h.

Keywords: transition zone design, differential settlement, voided sleepers, dynamic vehicle–track interaction, short-term performance, long-term performance.

1 Introduction

In transition zones between two different track forms, there is a discontinuity in the track structure leading to a gradient in track stiffness [1–5]. Examples include

transitions between different superstructures, for example slab track to ballasted track, and/or between different substructures, such as from an embankment to a bridge or tunnel structure. Differences and variations in loading and support conditions at the interfaces between the track superstructure and substructure on either side of the transition may result in differential track settlement, causing an irregularity in longitudinal rail level soon after construction. This irregularity leads to an amplification of the dynamic traffic loading along the transition, contributing to the degradation process of ballast and subgrade and a further deterioration of vertical track geometry. Consequently, the track adjacent to a transition is prone to deteriorate at an accelerating rate, necessitating more frequent track maintenance. In recent years, infrastructure managers and researchers have devoted increasing attention to understand and optimise the long-term performance of transition zones using both simulation models and field measurements [6].

In Europe, voided sleepers and deterioration of track geometry in transition zones incurs annual maintenance costs for track realignment of about 110 million euros, while in the USA the corresponding cost is around 200 million dollars [7,8]. It is argued that 75% of these costs is due to the consolidation of soil and compaction of ballast [7,8]. The track stiffness gradient between the two track forms also affects transition zone performance as influenced by track component design [4].

Different transition zone designs have been implemented in the field to mitigate the variations in loading and support conditions. Many of these solutions aim for a gradual and smoother variation in track stiffness from one track form to the other. Some approaches are designed to improve the support of the subgrade, while others focus on the superstructure including the implementation of specific track components such as wider sleepers, auxiliary rails and elastic pads (including conventional rail pads with different stiffness characteristics and/or under sleeper pads). A review of various transition zone designs can be found in [9,10].

In parallel, extensive research has focused on the modelling of long-term differential settlement in transition zones. A review of existing mechanistic-empirical settlement models can be found in [11]. A common technique is to adopt an integrated and iterative approach, where a model of the dynamic vehicle–track interaction in the short term is combined with an empirical model of the long-term settlement. For instance, Nasrollahi et al. [3] presented such a simulation method to predict the deterioration of track geometry due to differential settlement in the transition from a ballasted track to a Moulded Modular Multi-Blocks (3MB) slab track. In [12], this numerical approach was further improved by implementing a seven-parameter model of the ballast and subgrade to account for potential loss of contact between sleeper and ballast and the interaction between sleepers via the ground, and it was verified and calibrated using measured data from [5]. In [5], extensive measurements in a transition zone between a conventional ballasted track and a 48 m section of the 3MB slab track were carried out.

This paper presents a simulation study to demonstrate how reduced sleeper spacing and a broader sleeper base design could influence the long-term performance of a transition zone. The differential track settlement within the transition zone is predicted

using the iterative method from [3,12]. The calibrated non-linear finite element model includes the influence of gravity force on the superstructure, variable stiffness of the foundation, and the evolving occurrence of voided sleepers and redistribution of load on the foundation. The chosen settlement model is derived from a visco-plastic material mechanics model. An initial vertical rail misalignment between the two track forms, being a consequence of sleeper settlement due to the early stages of soil consolidation and ballast compaction, may also be considered.

2   Track and vehicle models

In this section, the 2D FE model of a transition zone for time-domain simulation of vertical dynamic vehicle–track interaction is briefly described, cf. Fig. 1. The track model is a non-linear FE model using beam elements for the rail and for the top blocks and base slab in the 3MB slab track. Each rigid sleeper is supported by a state-dependent seven-parameter model of the ballast and subgrade including a spring with bi-linear stiffness to represent the coupling (or void) between sleeper and ballast mass. It considers the interaction of interlocking ballast granules via a shear stiffness and shear damping coupling between neighbouring ballast masses. To reduce simulation time, symmetric vehicle and track properties with respect to a centre line between the two rails of the track are assumed. The model is described in more detail in [3,12].

The model has been calibrated using measured data. In [5], a real-time monitoring system was designed and used to assess the influence of traffic load on the accumulated differential settlement in a transition zone. The test site was located on the Swedish heavy haul line *Malmbanan* at Gransjö, north of Boden. The traffic on *Malmbanan*, a single-track railway line in northern Sweden, is dominated by iron ore freight trains with axle loads up to 32.5 tonnes and speeds 60 km/h (70 km/h in tare conditions). Extensive measurements were carried out in the transition zone between the conventional ballasted track and the 48 m section of a 3MB slab track. The monitoring took place from September 2022 to June 2023 using fibre grating sensors to measure axial rail strains (to assess rail bending moments) and vertical sleeper displacements relative to a fixed anchor. The long-term evolution of sleeper settlement was extracted from the measured sleeper displacements at times between train passages.

From the literature, typical lengths of transition zones are 5 – 30 m, cf. [13,14]. In technical reports from the UIC (International Union of Railways) [15] and the Swedish Transport Administration [16], the general recommendation is that the length of the transition should correspond to at least the distance the vehicles travel during half a second. In this study, the performance of the transition design when subjected to iron ore trains passing at speed 60 km/h and with axle loads of 30 tonnes is analysed. However, in the field, the same transition zone is used for other types of traffic. Since the maximum allowed train speed on the line is 135 km/h, the length of the transition zone studied here is 19 m. To limit the influence of effects from the boundaries of the track model on the dynamic response in the transition zone, the length of the section of ballasted track is taken as 45 m. The full track model represents a total length of 64.2 m (45 m of ballasted track and 19.2 m of 3MB slab track).

The ballasted track comprises 60 kg/m rails, rubber rail pads, and concrete sleepers designed for axle loads up to 35 tonnes. The rail is modelled with Euler-Bernoulli beam elements with bending stiffness ($EI_r = 6.4$ MNm^2) and mass per unit length ($m_r = 60$ kg/m) with four beam elements per sleeper bay. Each rail pad is modelled by a spring and viscous damper element. Each half sleeper in the ballasted track is a discrete (rigid) element with one vertical degree of freedom and nominal (reference) mass $m_s = 150$ kg. In this paper, sleeper (rail seat) distance L in the reference track model is assumed to be uniform with $L = 0.6$ m on both the ballasted and slab sides. The sleepers and rail seats in the ballasted track are numbered with index i ($i = 1, 2, \dots N_{bays}$-1: $i > 0$) starting from the transition, while the rail seats in the slab track are numbered as ($i = -1, -2, \dots: i < 0$), cf. Fig. 1.

The iron ore vehicle is represented by a rigid body model involving one car body and two three-piece bogies, each consisting of a bolster (in this model, rigidly connected to the car body), two side frames and two wheelsets. The vehicle model in Fig. 1 has 14 DOFs. The contact between each wheel and rail is modelled using a non-linear Hertzian spring. For more details and input to the model, see [3].
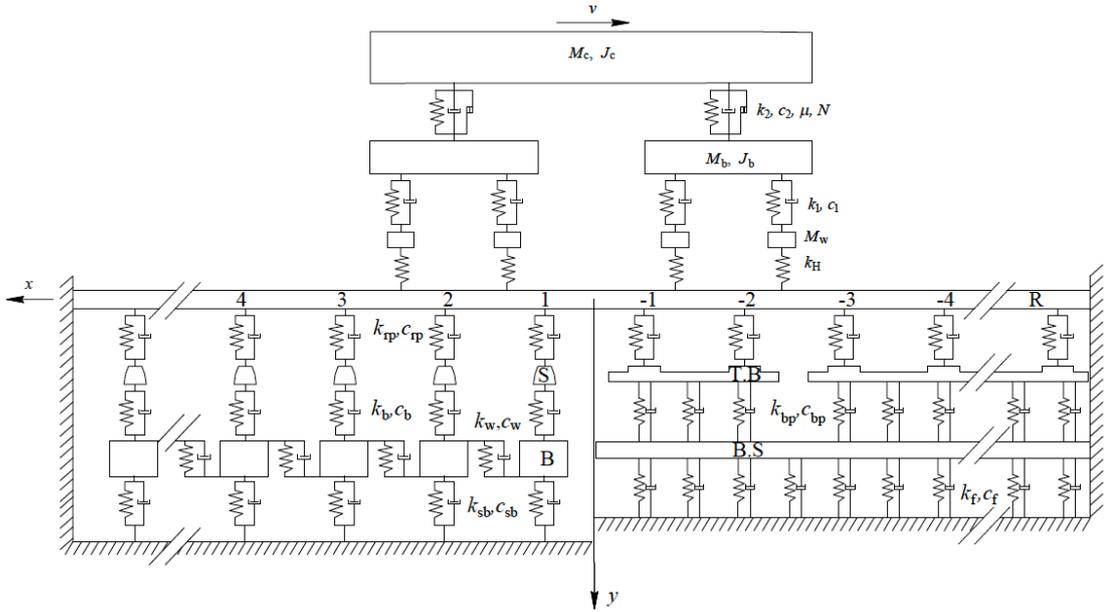

Figure 1: Sketch of complete vehicle and transition zone model: The sleepers (s) are rigid masses supported by a spring-damper connection (representing the ballast) with non-linear, and potentially random, stiffness properties, and ballast masses (B) supported by a spring-damper model representing the subgrade. Additionally, there is a spring-damper connection between adjacent ballast masses.

The full simulation model is based on an iterative approach where a time-domain model of vertical dynamic vehicle–track interaction in the short term (accounting for voided sleepers and state-dependent properties of the ballast and subgrade at each sleeper–ballast interface) is integrated with an empirical model of accumulated ballast and subgrade settlement in the long term [3]. In each iteration step, the pre-calculated static track displacement due to gravity load is used as initial conditions for the

simulation of vehicle–track dynamics. The maxima of the calculated contact pressure at the interface between each sleeper and ballast in the ballasted track section, generated by the combination of gravity load on the track superstructure and the load from each of the passing wheels of the vehicle model, are identified and used as input to the empirical settlement model. In each iteration step, the track model is updated to account for the current states of the support conditions. By taking several iteration steps, the accumulated differential settlement in the long term, the potential development of voided sleepers and the resulting redistribution of foundation loads between adjacent sleepers are calculated [3].

3   Settlement model

For a traffic load corresponding to a given number of load cycles (wheel passes), the long-term accumulated differential settlement and track geometry degradation in the transition zone is calculated using the iterative procedure. The empirical equation is based on a visco-plastic material mechanics model to calculate the settlement of each sleeper [4]. In each iteration step, after solving the short-term vehicle–track interaction problem, the time history of each sleeper–ballast contact pressure is calculated in a post-processing step. For each vehicle model passage in iteration step j $(j = 1, 2, \ldots n_\mathrm{s})$, the incremental settlement $\delta_{i,j}$ [m] at sleeper i $(i = 1, 2, \ldots N_\mathrm{bays}\text{-}1)$ is formulated as a function of the maxima of the sleeper–ballast contact pressure $p_{\mathrm{s/b},i}$. The model, which has been calibrated against the settlements measured at Gransjö [5,12], is written as

$$\delta_{i,j} = \sum_{n=1}^{N_\mathrm{w}} \left\{ \sum_{k=1}^{N_k} \alpha_k \left[\frac{\langle \max (p_{\mathrm{s/b},i})_n - p_{\mathrm{th},i} \rangle}{p_0} \right]^{\beta_k} \right\} \tag{1}$$

where N_w is the number of wheels in the vehicle model (here, $N_\mathrm{w} = 4$). Within each iteration step, it is assumed that the set of maximum contact stresses remains the same for all vehicle passes such that a linear extrapolation of each settlement increment to represent up to 10^5 load cycles (corresponding to $3 - 3.25$ MGT of traffic with loaded iron ore trains) can be carried out. However, an adaptive step length is applied such that a maximum allowed settlement increment $\delta^\mathrm{max} = 0.2$ mm per iteration step is allowed. If the increment exceeds δ^max, a linear interpolation is applied. The order N_k of the polynomial formulation and the corresponding parameters α_k and β_k are empirical, while $p_0 = 1$ kN/m^2 is a reference contact pressure with a unit such that the term within the square brackets becomes non-dimensional. Here, $N_k = 1$. In this settlement model, there is no accumulation of permanent ballast/subgrade deformation if the maximum sleeper–ballast contact pressure generated by a passing wheel is below a certain threshold value $p_{\mathrm{th},i}$ as reflected by the Macaulay brackets in Eq. (1).

The accumulated settlement at sleeper i after n_s iteration steps (corresponding to N_s wheel passes) is calculated by summing the incremental settlements calculated for each preceding step j

$$\Delta_i(n_s) = \sum_{j=1}^{n_s} \delta_{i,j} \tag{2}$$

In the next iteration step, the accumulated settlements are considered in the updated track model by implementing bi-linear stiffness characteristics for each sleeper–ballast coupling model. For each sleeper i, it is assumed that the current threshold value $p_{\text{th},i}$ is dependent on the accumulated settlement Δ_i as

$$p_{\text{th},i}(\Delta_i) = p_{\text{th},\infty} - \left(p_{\text{th},\infty} - p_{\text{th},0}\right)e^{-\gamma\Delta_i} \tag{3}$$

Here $p_{\text{th},0}$ is the reference threshold value before any traffic loading has been applied, $p_{\text{th},\infty}$ is the long-term threshold value corresponding to a completely stabilised track, while γ is a parameter that determines the rate of hardening. The parameters of the threshold value are track-site specific, see for example [12] where the settlement model was calibrated versus the measurements at Gransjö. Since it is argued that the conditions at Gransjö were particularly extreme, the following input data have been applied: $p_{\text{th},\infty} = 265$ kN/m^2, $p_{\text{th},0} = 103$ kN/m^2, $\gamma = 0.15$, $\alpha_1 = 0.007$ mm per 10^5 load cycles and $\beta_1 = 1.5$.

4   Results

The simulation procedure is demonstrated by calculating the track settlement adjacent to a transition between a ballasted track and a 3MB slab track due to an accumulated traffic load of 15 MGT, corresponding to one year of traffic with the loaded iron ore trains. Three different designs of the transition zone are compared, and the studied traffic direction is from ballasted track to slab track.

It is assumed that the bed modulus on the slab side is 300 (MN/m)/m^2, representing a very stiff foundation that for example could mimic the support conditions on a bridge or in a tunnel. This corresponds to a Winkler bed stiffness $k_f = 180$ (kN/mm)/m for the 3MB base slab, cf. Fig. 1. The remaining input parameters for the ballasted and slab track sections have been copied from the calibrated model, see [12]. An initial vertical rail misalignment due to early compaction of the ballast and consolidation of soil soon after construction of the transition zone is assumed by prescribing $\Delta_{\text{init}} = 2$ mm uniform settlement for all sleepers on the ballasted side in the first iteration.

The calculated track stiffness at rail level for the reference transition zone design is presented in Fig. 2. A significant stiffness gradient is observed at the transition. The combination of this stiffness gradient and the initial rail misalignment leads to a pitching motion of the two bogies and the car body resulting in a transient dynamic loading of the track and higher sleeper–ballast contact pressures close to the transition [3]. This leads to larger accumulated settlements for the sleepers adjacent to the transition, which in the long term can be observed as a local maximum in settlement

near the transition [3]. Two alternative transition zone designs have been implemented to mitigate the effect of the stiffness gradient. For sleepers ($i =$) $1 - 32$, these designs correspond to either implementing (Case 1) sleepers with a wider base or (Case 2) reducing the sleeper spacing. Both cases increase track stiffness at rail level on the ballasted side and leads to a more gradual (in two steps) change of track stiffness at rail level, see Fig. 2. For Case 1, the sleeper spacing for sleepers $1 - 32$ has been reduced from 0.60 m to 0.55 m. For Case 2, the nominal half sleeper base area (0.34 m^2) has been increased by 10%. Both cases lead to another stiffness gradient between the start of the transition zone and the conventional ballasted track design. Based on the simulation model, both Case 1 and Case 2 lead to lower sleeper–ballast contact pressures for sleepers $1 - 32$, cf. Fig. 3.

In Fig 4, the evolving sleeper settlement for sleepers 10 and 40 is shown for the different cases. Each iteration is indicated by a marker. As expected, for sleeper 40 outside of the transition zone, the sleeper settlement is similar for all cases. However, for sleeper 10, the transition zone designs (Cases 1 and 2) lead to a substantial reduction of settlement relative to the reference design.

The resulting longitudinal level (unloaded rail displacement) along the transition zone after 15 MGT is illustrated in Fig. 5. For the reference track model, there is a substantial dip in longitudinal level close to the transition due to the local maximum in the evaluated settlements, while the settlement far from the transition is uniform. Cases 1 and 2 lead to similar unloaded rail displacements outside of the transition zone but smaller displacements within the transition zone. In particular, using the Case 1 or Case 2 design leads to a significant reduction of the local maximum (dip) in settlement near the transition. Thus, it is argued that the implementation of a transition zone design according to Case 1 or Case 2 reduces the dynamic loading and improves the long-term performance of the transition. Based on the demonstrated simulation model, a further optimisation of the transition zone design can be carried out by for example combining the two cases and implementing variable characteristics along the transition.
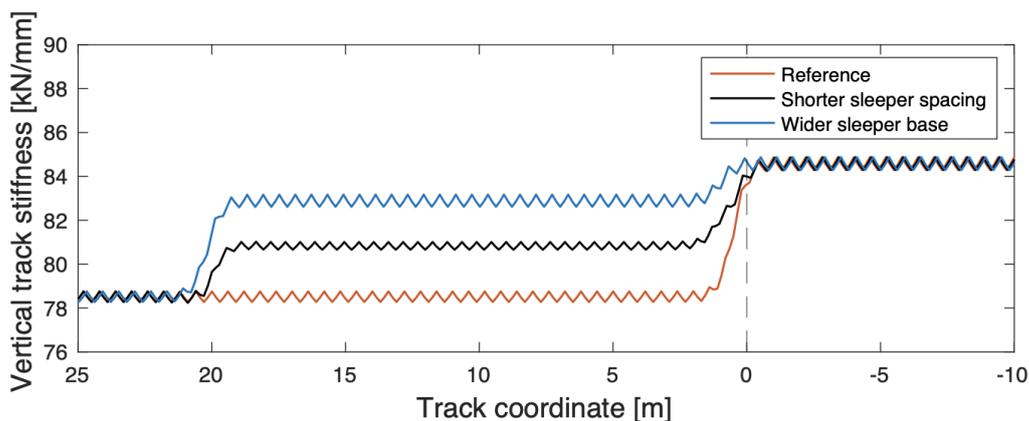

Figure 2: Static track stiffness at rail level along the transition using different transition zone designs on the ballasted side. Track coordinate is positive on the ballasted side, cf. Fig. 1. The oscillating character of the stiffness curves is due to the sleeper spacing.
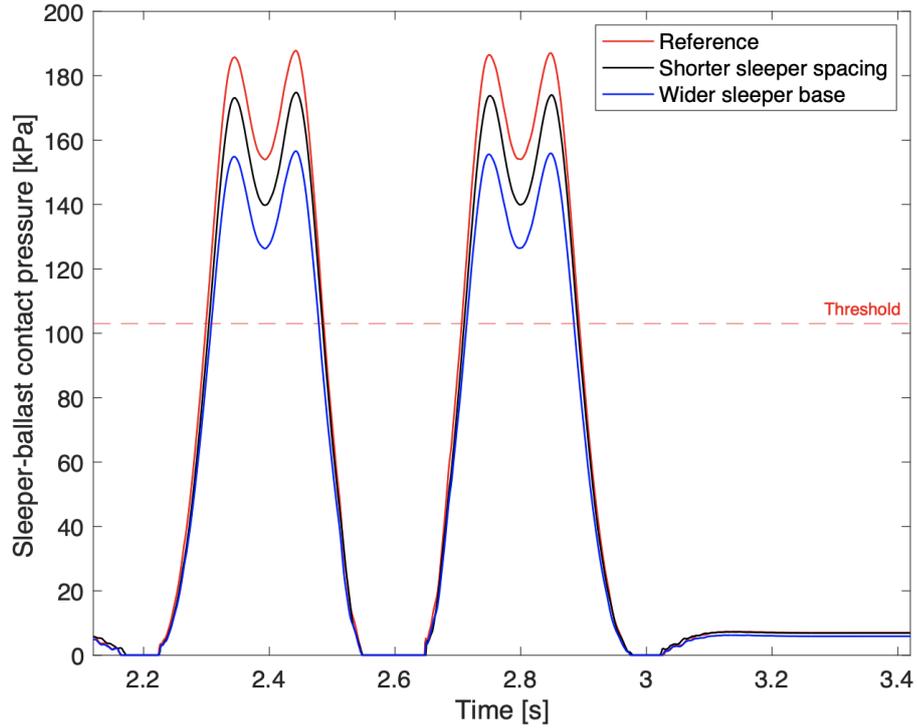
7

Figure 3: Time history of sleeper–ballast contact pressure at sleeper 10 using different transition zone designs on the ballasted side. Contact pressure 0 kPa indicates loss of sleeper–ballast contact. Iteration 1.
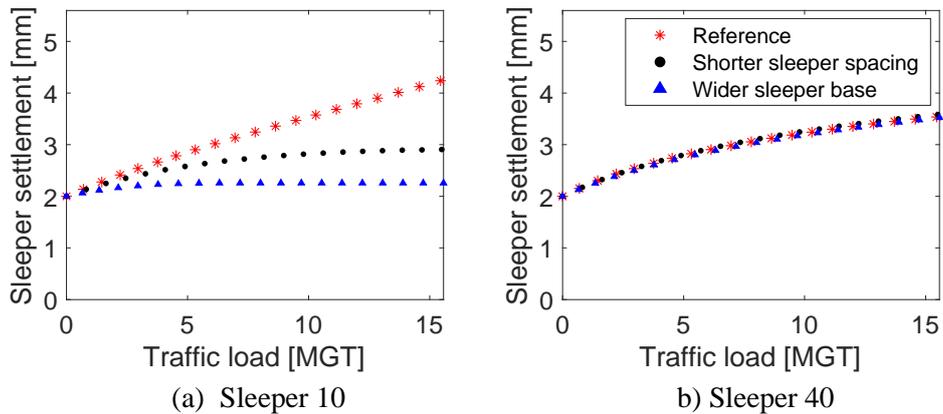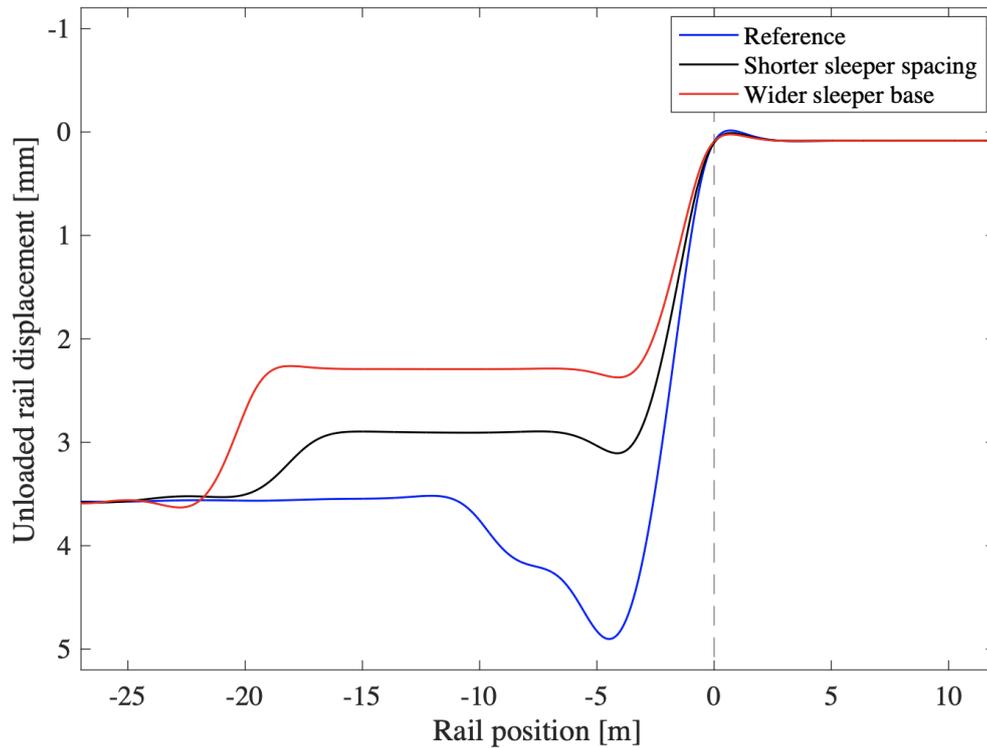

(a) Sleeper 10

b) Sleeper 40

Figure 4: Comparison of accumulated settlement for sleepers 10 and 40 for different transition zone designs after one year of traffic. Each iteration is indicated by a marker. Initial uniform settlement $\Delta_{\text{init}} = 2$ mm for all sleepers on the ballasted side.

Fig. 5. Influence of transition zone design on unloaded rail displacement due to gravity load on the track superstructure after an accumulated traffic load of 15 MGT. Initial uniform settlement $\Delta_{\text{init}} = 2$ mm for all sleepers on the ballasted side. Train speed 60 km/h.

5   Conclusions

An iterative procedure for the prediction of long-term degradation of longitudinal level due to accumulated settlement of ballasted track in a transition zone has been demonstrated. It has been shown that the differential settlement of sleepers near the transition is higher than elsewhere because sleeper–ballast contact pressures are higher and exceed the prescribed threshold value in the settlement model. To reduce dynamic loading and the evolving local maximum in settlement (dip in longitudinal level), particular attention should be given to the first 3 – 8 m from the transition between the two track forms. Implementing sleepers with a wider base or prescribing a shorter sleeper spacing are two examples of design that reduce the stiffness gradient in a transition from a stiffer track form, such as from a slab track on a bridge or in a tunnel. Based on the demonstrated model, a further optimisation of the stiffness profile along the track can be carried out.

Acknowledgment

References

[1] H. Wang, V. Markine. Modelling of the long-term behaviour of transition zones: Prediction of track settlement. Engineering Structures 156:294–304, 2018. https://doi.org/10.1016/j.engstruct.2017.11.038.

[2] G. Ognibene, W. Powrie, L. Le Pen, J. Harkness. Analysis of a bridge approach: Long-term behaviour from short-term response. Proceedings 15th International Conference on Railway Engineering 2019: 1-15.

[3] K. Nasrollahi, J.C.O. Nielsen, E. Aggestam, J. Dijkstra, M. Ekh. Prediction of long-term differential track settlement in a transition zone using an iterative approach. Engineering Structures 283: 115830, 2023. https://doi.org/10.1016/j.engstruct.2023.115830.

[4] A. Ramos, A. Gomes Correia, R. Calçada, D.P. Connolly. Ballastless railway track transition zones: An embankment to tunnel analysis. Transportation Geotechnics 33:100728, 2022. https://doi.org/10.1016/j.trgeo.2022.100728.

[5] K. Nasrollahi, J. Dijkstra, J.C.O. Nielsen. Towards real-time condition monitoring of a transition zone in a railway structure using fibre Bragg grating sensors. Transportation Geotechnics 44:101166, 2024. https://doi.org/10.1016/j.trgeo.2023.101166.

[6] T. Dahlberg. Railway track stiffness variations - Consequences and countermeasures. International Journal of Civil Engineering 8:1–12, 2010.

[7] E. Tutumluer, T.D. Stark, D. Mishra, J.P. Hyslip. Investigation and mitigation of differential movement at railway transitions for US high speed passenger rail and joint passenger/freight corridors. ASME/IEEE Joint Rail Conference. American Society of Mechanical Engineers, 2012:75–84.

[8] J.E. Nicks. The bump at the end of the railway bridge. PhD Thesis. Texas A&M University, Texas, United States, 2009.

[9] R. Sañudo, L. Dell'Olio, J.A. Casado, I.A. Carrascal, S. Diego. Track transitions in railways: A review. Construction and Building Materials 112:140–57, 2016. https://doi.org/10.1016/j.conbuildmat.2016.02.084.

[10] B. Indraratna, M. Babar Sajjad, T. Ngo, A. Gomes Correia, R. Kelly. Improved performance of ballasted tracks at transition zones: A review of experimental and modelling approaches. Transportation Geotechnics 21:100260, 2019. https://doi.org/10.1016/j.trgeo.2019.100260.

[11] T. Abadi, L. Le Pen, A. Zervos, W. Powrie. A review and evaluation of ballast settlement models using results from the Southampton Railway Testing

Facility (SRTF). Procedia Engineering, vol. 143, Elsevier B.V., p. 999–1006, 2016. https://doi.org/10.1016/j.proeng.2016.06.089.

[12] K. Nasrollahi, A. Ramos, J.C.O. Nielsen, J. Dijkstra, M. Ekh. Benchmark of calibrated 2D and 3D models for simulation of differential settlement in a transition zone using field measurement data. 2024 (submitted for international publication).

[13] P. Galvín, A. Romero, J. Domínguez. Fully three-dimensional analysis of high-speed train-track-soil-structure dynamic interaction. Journal of Sound and Vibration 329:5147–63, 2010. https://doi.org/10.1016/j.jsv.2010.06.016.

[14] M. Shahraki, C. Warnakulasooriya, K.J. Witt. Numerical study of transition zone between ballasted and ballastless railway track. Transportation Geotechnics 3:58–67, 2016. 10.1016/j.trgeo.2015.05.001.

[15] M. Fumely, G. Corzo Uceda, S. Crail, R. Haksel, C. Hofmann, F. Klösters, M. Missler, J. Mys, R. Potvin, R. Schilder, M. Testa, and J.-M. Trevin. Vertical elasticity of ballastless track. Technical report, the International Union of Railways (UIC), 2008.

[16] R. Karlsson, "Tekniska Systemkrav För Ostlänken" (Technical System Requirements for Ostlänken, in Swedish), version 2.0, published by Trafikverket in 2014.